

Investigation of Structural Characteristics of Bis(β -diketonato)copper(II) Complexes Containing Alkoxy or Aryloxy Side Chains: X-Ray Structures of 1,3-Bis(4-butoxyphenyl)propane-1,3-dione, Bis[1,3-bis(4-butoxyphenyl)propane-1,3-dionato- $\kappa O, \kappa O'$]copper(II) and Bis[1,3-bis(4-phenoxyphenyl)propane-1,3-dionato- $\kappa O, \kappa O'$]copper(II)

by José A. Campo^a), Mercedes Cano^a)*, José V. Heras^a), M. Cristina Lagunas^a), Josefina Perles^a),
Elena Pinilla^a)^b), and M. Rosario Torres^b)

^a) Departamento de Química Inorgánica I, Facultad de Ciencias Químicas, Universidad Complutense,
E-28040 Madrid (e-mail: mmcano@ucmax.sim.ucm.es)

^b) Laboratorio de Difracción de Rayos-X, Facultad de Ciencias Químicas, Universidad Complutense,
E-28040 Madrid

Copper(II) complexes containing β -diketonato ligands of the general formula $[\text{Cu}\{(4\text{-RO})\text{C}_6\text{H}_4\text{COCH}_2\text{COC}_6\text{H}_4(4\text{-OR})\}_2]$ **3** (R = Bu) or **4** (R = Ph) were prepared and their structures solved by X-ray diffraction. The crystal structure of the parent ligand $(4\text{-BuO})\text{C}_6\text{H}_4\text{COCH}_2\text{COC}_6\text{H}_4(4\text{-OBu})$ **1** was also solved. The influence of the different side chains $4\text{-RO}-\text{C}_6\text{H}_4$ (R = Bu or Ph) on potential liquid-crystal properties was investigated for both the ligands and the copper derivatives. The presence of BuO substituents at the aromatic rings appears to improve the molecular linearity with respect to 1,3-diphenylpropane-1,3-dione (= dibenzoylmethane; DBM), this feature being of interest for rod-like structures. On the other hand, the molecular structure of the copper(II) complexes **3** and **4** showed a flat core almost unmodified by the different peripheral substituents. A columnar arrangement was observed for both compounds **3** and **4**, but, additionally, a layer-like disposition was also found in **3**, which was proved to be a metallomesogen.

Introduction. – The development of new molecular structures suitable for technological applications is one of the main goals of research in the field of molecular-based materials. In this sense, the synthesis of metallomesogenic compounds has significantly grown in recent years, but the control and understanding of the liquid-crystalline state still require new efforts [1–5].

X-Ray studies of the mesophases have been reported [1–10]. By contrast, although a recent review dealing with X-ray crystal structures of organic mesogenic compounds has been published by Haase and Athanassopoulou [11], the analyses of metallomesogens in the solid state have received less attention [1–4]. Because we believe that the study of single crystals could give insight into intermolecular interactions that may enhance mesomorphism, the main goal of our work was to investigate the potential relationships between the X-ray structures and the mesogenic behavior.

(β -Diketonato)metal complexes containing side-chain substituents at the ligands are among the best known disc-shaped coordination compounds exhibiting liquid-crystal properties, and the importance of electronic factors in the mesophase formation has been evidenced in many of them [1–4][10][12–15]. It has also been observed that most of these (β -diketonato)copper(II) complexes exhibit crystalline polymorphism, which is a very common characteristic of mesogenic and promesogenic compounds

[1–4][8][16–23]. However, structural data for this type of compounds are rather scarce [1–4][24–29]. There has, despite this, been some interest in the structure of the free β -diketone ligands because of the influence of intramolecular H-bonds on the crystal packing and/or in determining electronic and conformational properties [13][30–32].

According to literature data, double melting has been observed for 1,3-bis(4-butoxyphenyl)propane-1,3-dione (**1**), behavior that is closely associated with mesomorphism [30]. Indeed, the related Cu complex bis[1,3-bis(4-butoxyphenyl)propane-1,3-dionato- $\kappa O, \kappa O'$]copper(II) (**3**) showed discotic mesomorphism [19].

With these precedents in mind, we describe herein the crystal structures of the promesogenic diketone ligand **1** and its mesogenic related (diketonato)copper complex **3**. In addition, the new ligand 1,3-bis(4-phenoxyphenyl)propane-1,3-dione (**2**) and its Cu derivative bis[1,3-bis(4-phenoxyphenyl)propane-1,3-dionato- $\kappa O, \kappa O'$]copper(II) (**4**) were also prepared and their properties analyzed. The crystal structure of **4** was also determined for comparative purposes, as well as to illustrate the influence of aromatic-ether groups on the chelate ring.

Results and Discussion. – *Synthetic Studies and Properties.* The β -diketone ligands **1** and **2** were prepared by a condensation reaction between the corresponding substituted acetophenone and ethyl benzoate as previously described for other diketones (*Scheme*) [13, 18, 32]. The starting compounds, ethyl 4-phenoxybenzoate and ethyl 4-butoxybenzoate, were prepared and characterized as described in the *Exper. Part*. The diketones **1** and **2** were fully characterized, and their IR and NMR data (*Table 1*) indicate that they are mostly present as the enol isomer in both solid state and solution. The $^1\text{H-NMR}$ spectra clearly show two signals at *ca.* 6.70 and 4.50 ppm assigned to the CH and CH_2 protons of the enol and keto forms, respectively, in a ratio of 95:5. The resolution of the crystal structure of **1** confirms the existence of the enol form in the solid state as described below.

Reactions of **1** and **2** with copper(II) acetate gave the corresponding (β -diketonato)copper complexes **3** and **4** (*Scheme*) by an alternative method to that described in the literature [17][18]. The analytical and IR data (see *Exper. Part*) are in agreement with the proposed structures.

The magnetic susceptibilities of **3** and **4** were measured over the range 2–300 K. These compounds followed a *Curie* law with magnetic moments of 1.83 and 1.70 MB, respectively. These values were in the expected range for a Cu^{II} ion ($S=1/2$) with isolated spins [21].

The mesomorphism of **3** has already been published by *Ohta et al.*, as part of the study of a family of (diketonato)copper complexes containing from 1 to 12 C-atoms in the alkyl side chains R [19]. For **3**, two crystalline phases and a discotic mesophase were found and the transition temperatures determined [19]. We have now obtained single crystals of **3**, and again investigated their thermal behavior by polarizing microscopy and differential scanning calorimetry (DSC). DSC revealed endothermic transitions at 171, 183, and 210° (*Table 2*), the phase between 171 and 210° being a discotic mesophase, in agreement with that previously reported [19]. The texture change from the crystal phase to the discotic mesophase was clearly observed in both the heating and cooling stages, the discotic phase exhibiting a mosaic texture as shown in the photomicrograph in *Fig. 1*. Phase transformations of ligands **1** and **2**, and complex **4**

Scheme

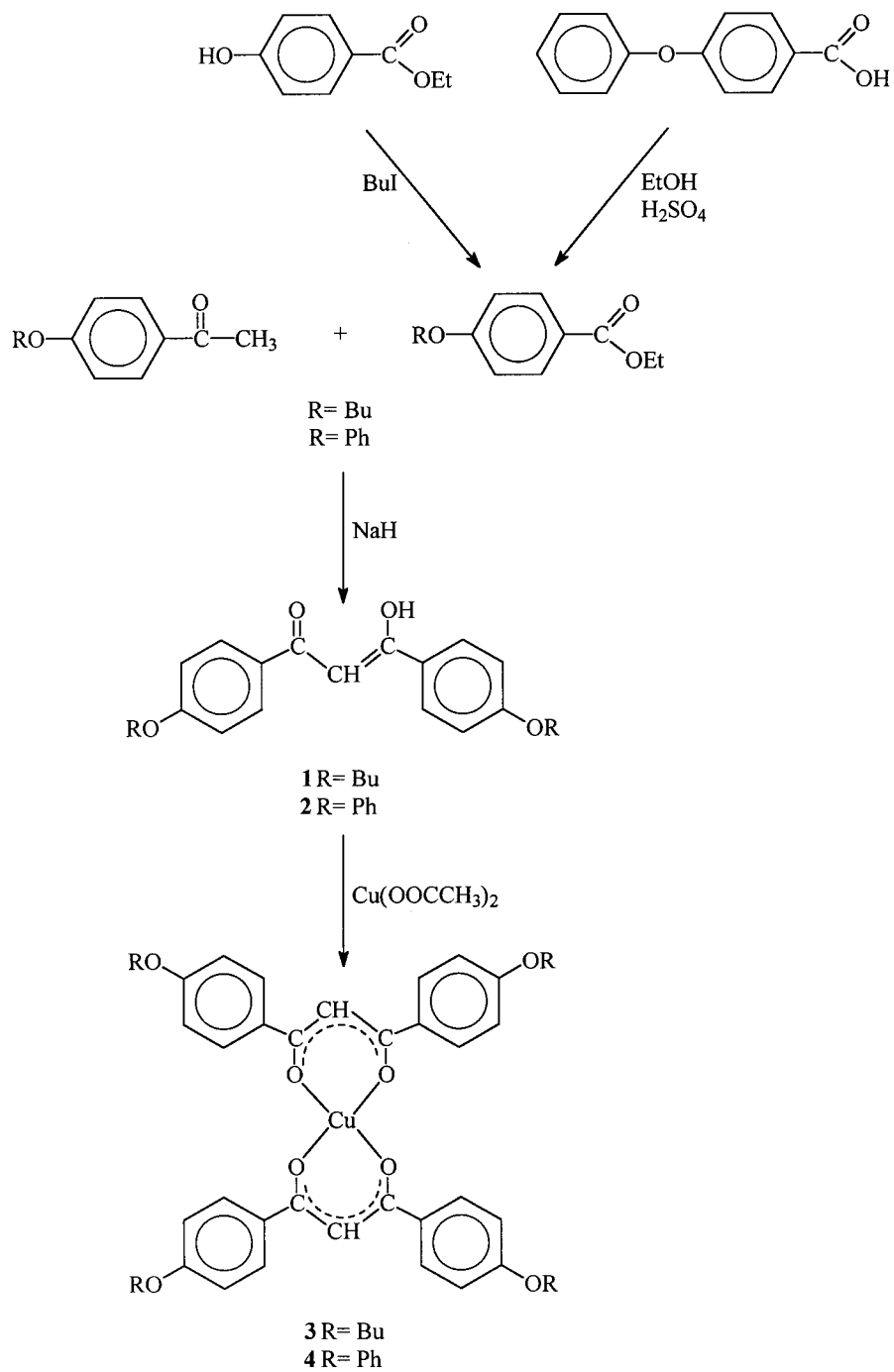


Table 1. IR and NMR Data for the β -Diketones **1** and **2**

		1	2
IR ^{a)} ($\bar{\nu}$ in cm ⁻¹)	C=O	1602	1606
	C=C	1587	1589
¹ H-NMR ^{b)} ^{c)} (δ in ppm, J in Hz)	CH [CH ₂]	6.71 (s) [4.53 (s)]	6.76 (s) [4.56 (s)]
	C ₆ H ₄	7.92, 6.93 (2d); $J=9$	7.97 (d), 7.09 (m); $J=9$
	R	4.01 (t), 1.78 (q), 1.49 (sext.), 0.97 (t); $J=7$	7.42 (t), 7.21 (m), 7.09 (m); $J=8$
¹³ C-NMR ^{b)} ^{c)} (δ in ppm)	CO	184.5	184.5
	CH	91.3	92.0
	C ₆ H ₄	162.6, 129.0, 127.9, 114.3	162.0, 155.7, 131.5, 130.0
	R	67.9, 31.1, 19.1, 13.8	129.1, 124.4, 120.0, 117.6 ^{d)}

^{a)} KBr discs. ^{b)} CDCl₃ solution at room temperature. ^{c)} The data are those of the enol isomer; only the δ (H) of the CH₂ protons of the keto form is given in brackets. Other small signals observed are attributed to the resonances of the keto isomer. ^{d)} The δ (C) of the PhOC₆H₄ groups are listed but not assigned.

Table 2. Phase Properties of Compounds **1–4**

	Transition	T [°]	ΔH [kJ mol ⁻¹]
1 ^{a)}	K → IL	92	41.8
2	K → IL	126	25.4
3 ^{b)}	K ₁ → D	171	2.3
	K ₂ → D	183	16.7
	D → IL	210	35.1
4	K → IL	253	84.8

^{a)} A double melting point has previously been found for this compound and related to the presence of two K₁ and K₂ crystalline forms with a K₁ → K₂ transformation at *ca.* 17° [30]. ^{b)} These data are similar to those previously reported [19].

were also observed by polarizing microscopy and DSC. However, none of them showed thermotropic liquid-crystal behavior, and only a transformation to the isotropic liquid was detected. Table 2 shows the phase properties of compounds **1–4**.

X-Ray Study of 1. Fig. 2 shows an ORTEP perspective of **1** with the atomic numbering scheme. Table 3 lists selected bond distances and angles. Compound **1** is present in the enol form, which shows an almost linear geometry. The enol proton is located asymmetrically between the two O-atoms through a H-bond, an arrangement that is less symmetrical than that found in 1,3-diphenylpropane-1,3-dione (DBM) [33] (see Fig. 3). Other small differences between the two structures occur in the dihedral angles between the best least-squares planes of the central H-bonded ring C(1)–C(2)–O(1)–H(2)–O(2)–C(13) and the aryl-substituent rings: 12.0(1) and 4.9(2)° in **1**, and 17 and 4° in DBM. Therefore, an increased planarity together with a lower H-bond strength appear to be consequences of the butoxy substituents at the 4-position of the phenyl rings.

On the other hand, to explain the promesogenic behavior of diketone **1**, we investigated the molecular linearity that should favor rod-like calamitic mesophases.

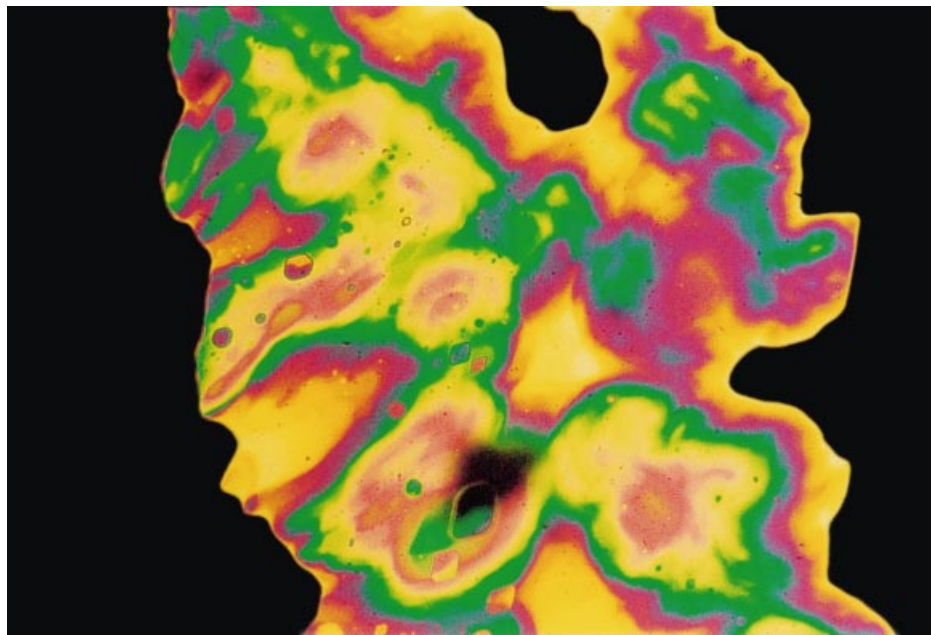


Fig. 1. Photomicrograph of the texture of the mesophase of compound **3** at 194°

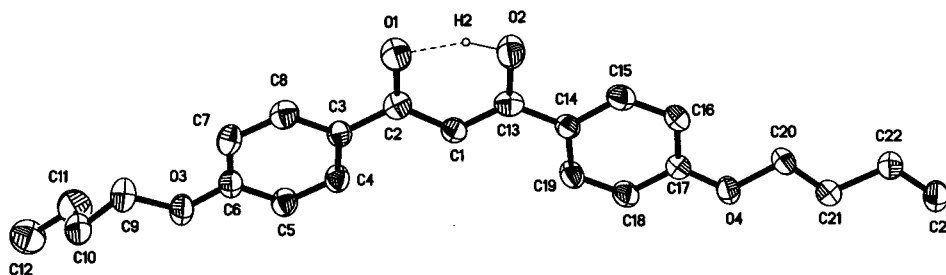


Fig. 2. Perspective ORTEP plot of **1** (R = Bu) showing the atomic numbering scheme. H-Atoms, except H(2) are omitted for clarity, and thermal ellipsoids are at 40% probability level.

The α angle, as defined in Fig. 4, is a measure of the linearity of the molecule. This angle is *ca.* 10° greater in **1** than in the unsubstituted diketone DBM [33], *i.e.* the presence of side chains on the aromatic rings improves the linearity. This indicates a potential for calamitic mesogens.

A view of the crystal packing through the z axis is shown in Fig. 5. This packing is similar to that in the stable form of DBM, showing a molecular ‘crossing’ of pairs of molecules, in contrast to the parallel disposition observed in the unstable form of DBM [33]. Short intermolecular contacts are found in **1**; thus, the distance between the keto atom O(1) and the atom C(4′) of a neighboring molecule is 3.274(4) Å. In addition, the distance O(1)⋯C(1′) is 3.876(4) Å, this interaction being slightly longer than that found in the stable form of DBM (3.70 Å), which was associated with a weak

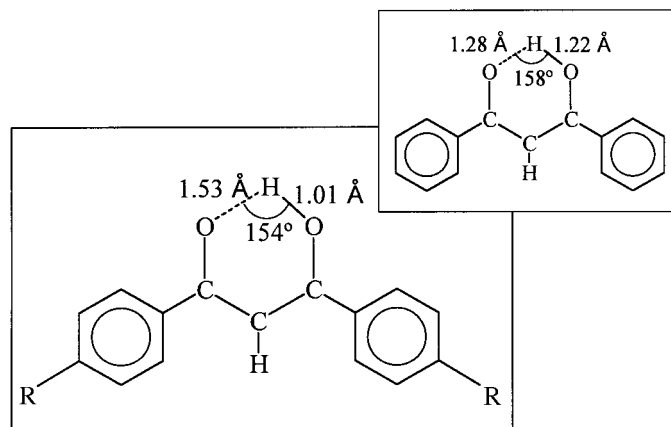


Fig. 3. Hydrogen-bond geometry for the enol ring of **1**. In the inset, the DBM molecule for comparison [33].

Table 3. Selected Bond Lengths [Å] and Angles [°] for **1**, **3**, and **4**^a). Arbitrary numbering.

1	O(1)–C(2)	1.290(3)	O(2)–H(2)	1.02(2)
	O(2)–C(13)	1.315(3)	O(1)⋯H(2)	1.52(2)
	C(1)–C(13)	1.376(3)	O(1)⋯O(2)	2.479(2)
	C(1)–C(2)	1.414(3)		
	C(13)–C(1)–C(2)	122.1(2)	C(13)–O(2)–H(2)	105(1)
	O(1)–C(2)–C(1)	119.8(2)	O(1)⋯H(2)–O(2)	153(2)
	C(1)–C(13)–O(2)	119.8(3)	C(2)–O(1)⋯H(2)	100.0(8)
3	Cu(1)–O(1)	1.895(3)	O(6)–C(36)	1.277(4)
	Cu(1)–O(6)	1.897(3)	C(24)–C(25)	1.388(5)
	Cu(1)–O(2)	1.902(3)	C(24)–C(36)	1.393(5)
	Cu(1)–O(5)	1.911(3)	Cu(2)–O(9)	1.891(3)
	O(1)–C(2)	1.280(5)	Cu(2)–O(10)	1.903(3)
	C(1)–C(13)	1.396(5)	O(9)–C(48)	1.278(5)
	C(1)–C(2)	1.390(5)	O(10)–C(59)	1.272(5)
	O(2)–C(13)	1.270(4)	C(47)–C(48)	1.395(6)
	O(5)–C(25)	1.274(4)	C(47)–C(59)	1.399(6)
	O(1)–Cu(1)–O(6)	179.3(1)	O(6)–Cu(1)–O(5)	93.3(1)
	O(1)–Cu(1)–O(2)	92.8(1)	O(2)–Cu(1)–O(5)	179.9(2)
	O(6)–Cu(1)–O(2)	86.8(1)	O(9)–Cu(2)–O(10')	86.8(1)
	O(1)–Cu(1)–O(5)	87.2(1)	O(9)–Cu(2)–O(10)	93.2(1)
4	Cu(1)–O(1)	1.902(2)	O(1)–C(2)	1.276(3)
	Cu(1)–O(2)	1.916(2)	O(2)–C(15)	1.278(3)
	Cu(1)–O(1')	1.902(2)	C(1)–C(2)	1.394(3)
	Cu(1)–O(2')	1.916(2)	C(1)–C(15)	1.395(4)
	O(1)–Cu(1)–O(2)	93.18(7)	O(1)–Cu(1)–O(2')	86.82(7)

^a) Symmetry transformations used to generate equivalent atoms ('): $-x+1, -y+1, -z$.

intermolecular H-bond and responsible for the molecular 'crossing' [33]. For **1**, the similar orientation of the molecules is probably due to both intermolecular interactions O(1)⋯C(4') and O(1)⋯C(1') and, therefore, could explain the lack of mesogenic behavior.

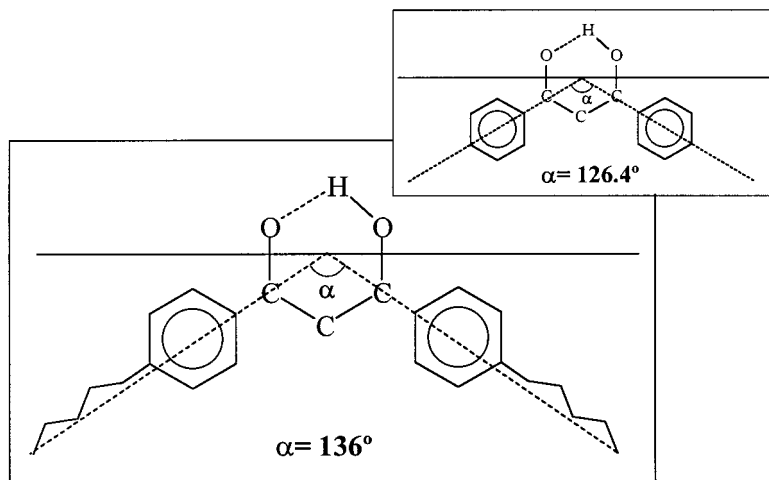


Fig. 4. *Molecular linearity for 1*. In the inset, the DBM molecule for comparison [33]. The α angle is defined as the angle between the lines connecting the keto C-atom and the last C-atom of the chain.

X-Ray Studies of 3 and 4. The crystal structure of bis[1,3-bis(4-butoxyphenyl)propane-1,3-dionato- $\kappa O, \kappa O'$]copper(II) (**3**), for which discogenic behavior has previously been described, is now presented. Also, the X-ray crystal structure of the related bis[1,3-bis(4-phenoxyphenyl)propane-1,3-dionato- $\kappa O, \kappa O'$]copper(II) (**4**) is described and compared with that of **3**. Figs. 6 and 7 show ORTEP perspectives of one of the crystallographically independent molecules of **3** (labelled as molecule *1*) and **4**, respectively, with the atomic numbering scheme. Selected bond lengths and angles are collected in *Table 3*.

Compound **3** has one molecule and half a molecule in the asymmetric unit (labelled as *1* and *2*), consistent with two Cu atoms, Cu(1) and Cu(2), in different crystallographic sites, the Cu(2) atom being located at a center of symmetry. The Cu atoms are surrounded by four O-atoms in a square planar arrangement with the Cu(1)–O and Cu(2)–O distances averaging 1.901(3) and 1.897(3) Å, respectively. For compound **4**, only half a molecule is found in the asymmetric unit with the Cu-atom located at a center of symmetry and coordinated to two O-atoms; therefore, the two centrosymmetric O-atoms complete the same planar coordination around the metal with Cu–O distances averaging 1.909(2) Å. The cores of molecules **3** and **4**, consisting of the CuO₄ unit and the six aliphatic C-atoms, are both nearly planar.

For **3**, the best least-squares planes through the Cu(1) atom, Cu(1)–O(1)–C(2)–C(1)–C(13)–O(2) and Cu(1)–O(5)–C(25)–C(24)–C(36)–O(6), makes an angle of 2.8(2)°. In addition, the best least-squares coordination planes of Cu(1) and Cu(2), defined by the corresponding four O-atoms and the Cu-atom, give a dihedral angle of 4.3(2)°. Therefore, the cores of both molecules are almost parallel. The aromatic rings are tilted with respect to the coordination planes, and the dihedral angles between these planes range from 2.4(1) to 16.7(1)° and 7.4(2) to 13.3(2)° for the molecules *1* and *2*, respectively.

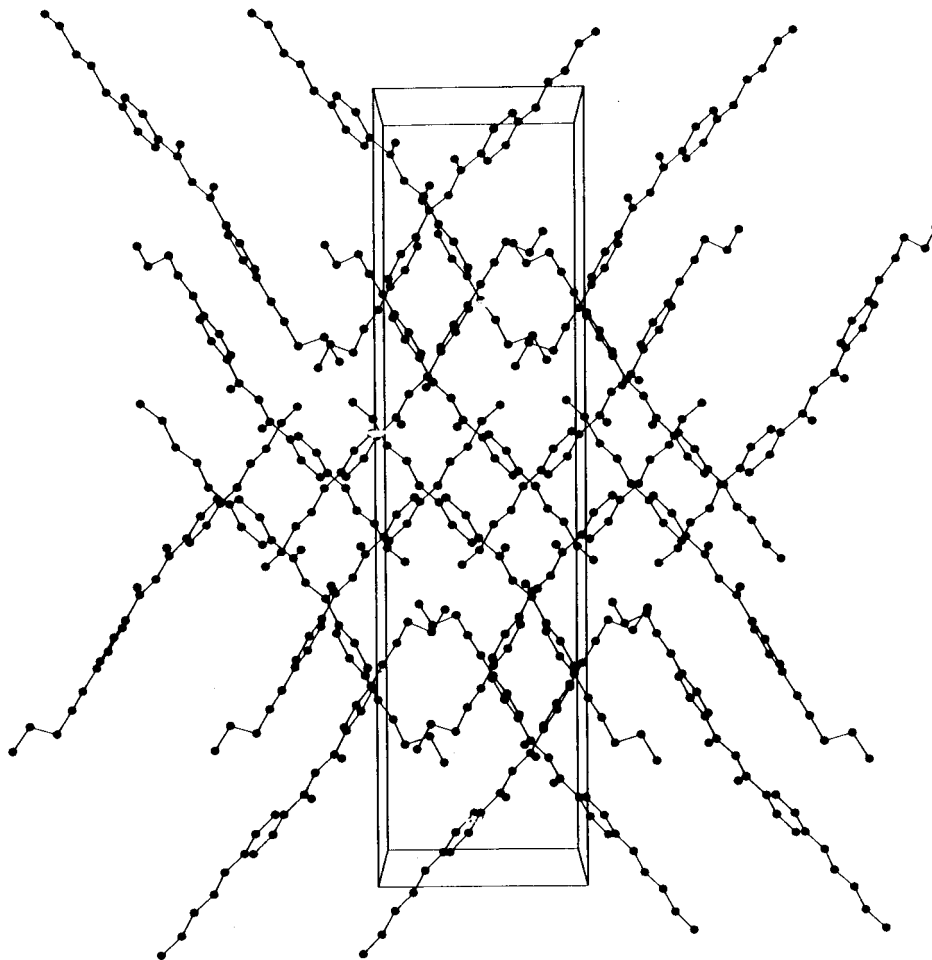


Fig. 5. Packing arrangement of **1** through the *z* axis

The principal structural features of the core of **3** are maintained for compound **4**. In particular, the central plane Cu(1)–O(1)–C(2)–C(1)–C(15)–O(2) and the two symmetry-unrelated aromatic groups are tilted at 4.5(1) and 8.7(1)°. However, the presence of the phenoxy substituents at the phenyl rings of the core results in a greater deviation from planarity, the dihedral angles between each pair of adjacent aromatic rings bonded by O-atoms (C₆H₅OC₆H₄) being 70.6(1) and 75.8(1)°.

In both structures, **3** and **4**, columnar characteristics are found. In addition, the molecular arrangement in **3** can be described as essentially layer-like (Fig. 8). Each molecule in the layer of **3** is surrounded by six others situated at $\pm c$, $\pm(a+b)$ and $\pm(a+b+c)$, with only interactions of the *Van der Waals*' type (the shortest intermolecular distance is between O(8) and C(5') at 3.537(5) Å). Layers of this type also have the molecules stacked in a columnar arrangement along the crystallographic

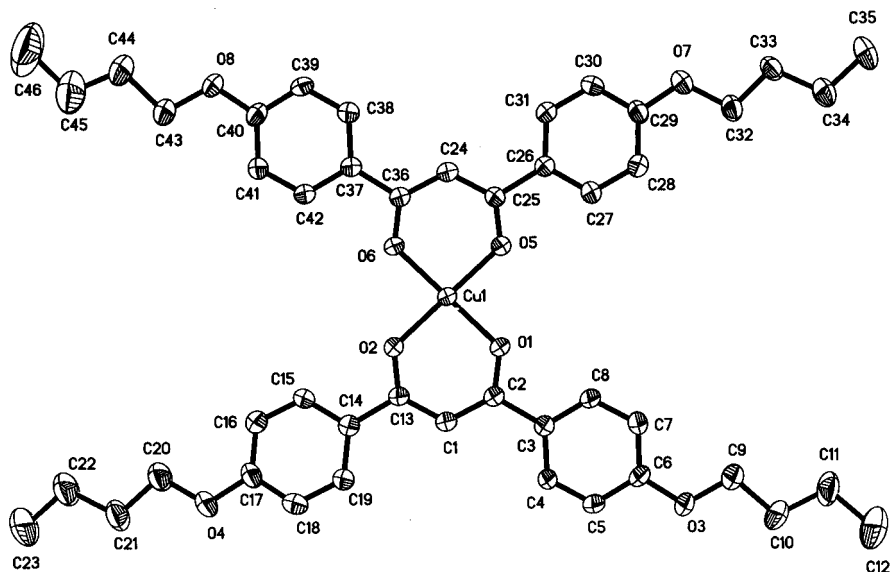


Fig. 6. *Perspective ORTEP plot of 3 (molecule 1)*. H-Atoms are omitted for clarity, and thermal ellipsoids are at 40% probability level.

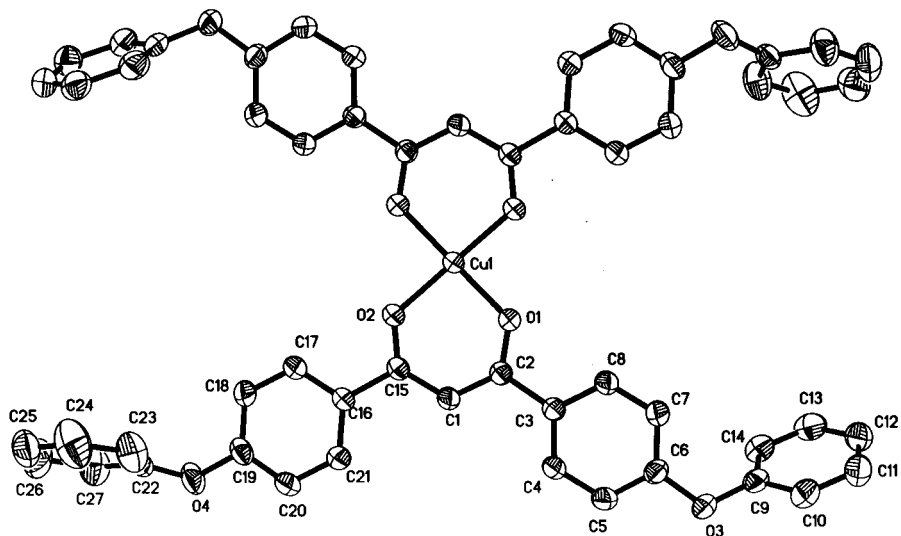


Fig. 7. *Perspective ORTEP plot of 4*. H-Atoms are omitted for clarity, and thermal ellipsoids are at 40% probability level.

b-axis. The core of the molecule is tilted with respect to the column axis by 54.4(1) and 53.0(1)° for Cu(1) and Cu(2), respectively. The Cu-atoms along the column axis are arranged in a zig-zag fashion with alternating steps of three and two atoms (*Fig. 9,a*). The zig-zag angle is 124°, and the Cu...Cu distances are 6.463(1) and 6.322(1) Å for

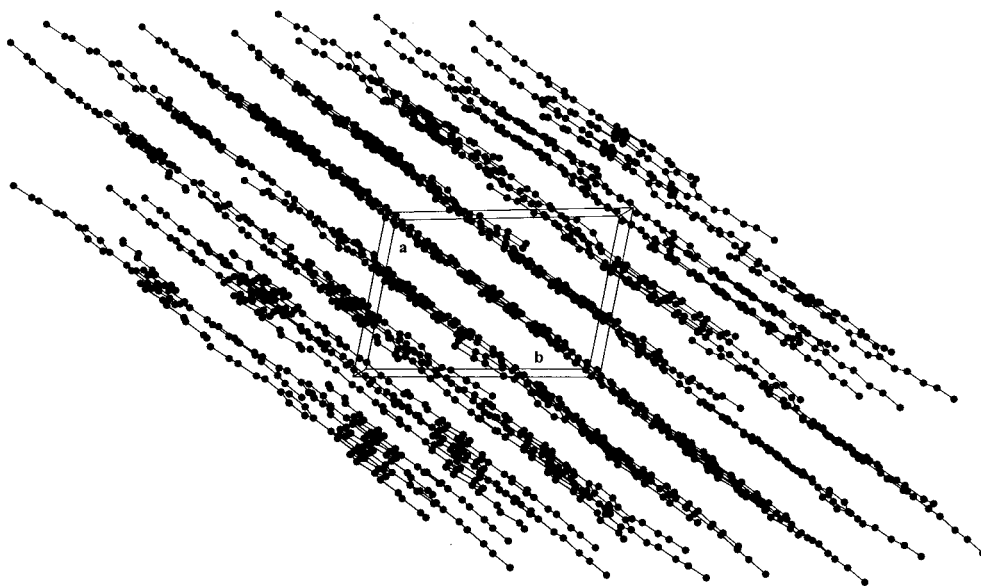


Fig. 8. Molecular arrangement of **3**

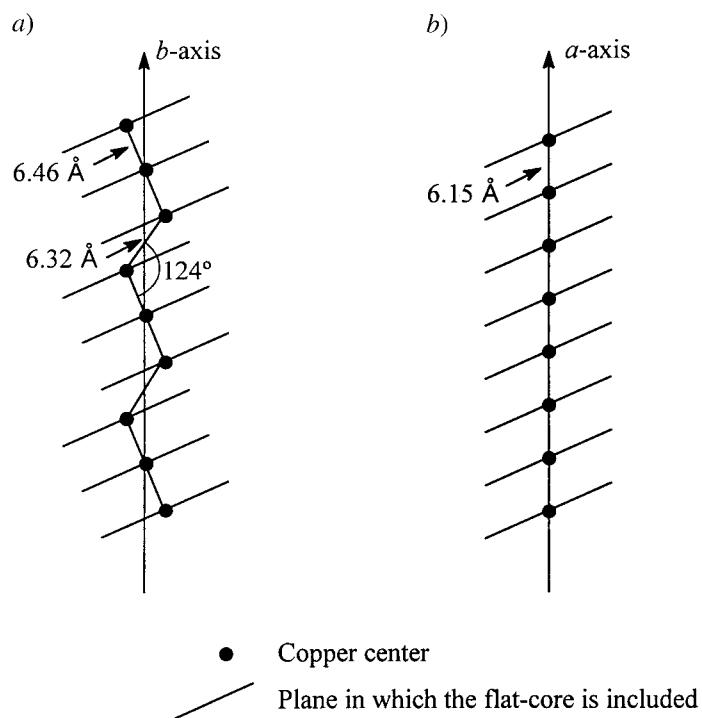


Fig. 9. Schematic representation of the columnar stacking in a) **3** and b) **4**

Cu(1)⋯Cu(2) and Cu(1)⋯Cu(1'), respectively. Each column in the crystal is surrounded by six others at $\pm a$, $\pm c$ and $\pm(a+c)$ in a distorted hexagonal arrangement. In compound **4**, the columnar stacking is observed along the crystallographic *a*-axis. In this case, the planar core of the molecule forms an angle of $121.28(3)^\circ$ with the columnar axis. The Cu-atoms adopt a linear disposition with a Cu⋯Cu distance of $6.1533(1) \text{ \AA}$ (Fig. 9, b).

The general structural features for **3** are related to those previously observed in other metallomesogenic (diketonato)copper complexes such as bis{1,3-bis[4-(octyloxy)phenyl]propane-1,3-dionato- $\kappa O, \kappa O'$ }copper(II), bis[1,3-bis(4-octylphenyl)propane-1,3-dionato- $\kappa O, \kappa O'$]copper(II), and {1,3-bis[4-(heptyloxy)phenyl]propane-1,3-dionato- $\kappa O, \kappa O'$ }[1,3-bis(4-heptylphenyl)propane-1,3-dionato- $\kappa O, \kappa O'$]copper(II) [24–28]. In all of these cases, the rigid cores of the molecules are surrounded by a fringe of flexible chains, with the fringes of neighboring columns interpenetrating. By contrast, the most singular structural characteristic in **4** is the absence of a layer-like molecular arrangement, with the cores between neighboring columns tilted at $79.02(6)^\circ$ (Fig. 10). This fact is related to the presence of the phenoxy substituents, which, in turn, could be responsible for the nonmesogenic behavior of **4**. It is also interesting to note that compound **4** crystallizes in the $P2_1/n$ space group, in contrast to the above related mesogenic compounds (space group $P\bar{1}$).

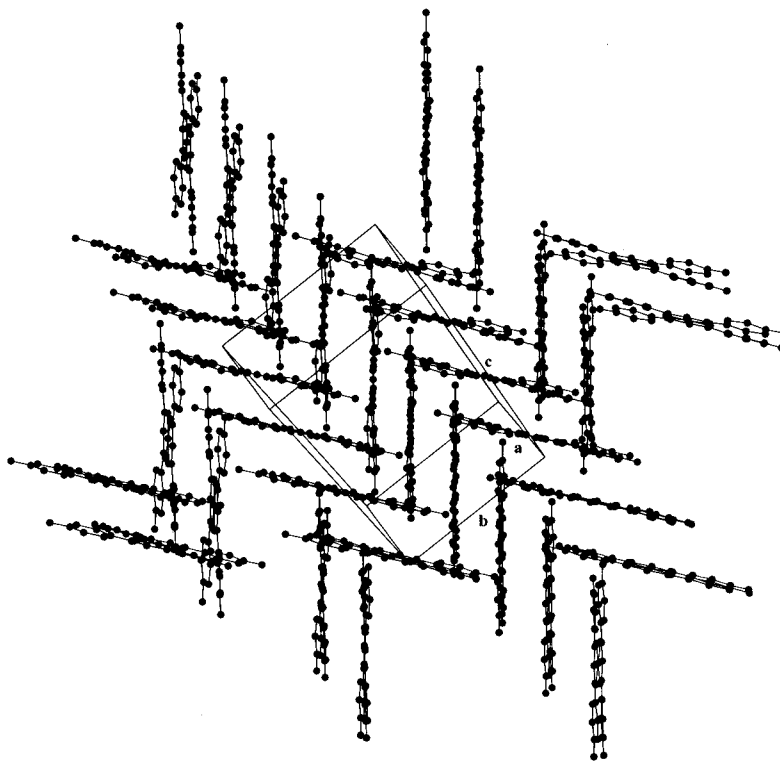


Fig. 10. Molecular arrangement of **4**. The Ph groups are omitted for clarity.

Conclusions. – (Aryloxy)phenyl or (alkyloxy)phenyl substituents at the 1 and 3 positions of β -diketone ligands **1** and **2** do not modify the structural characteristics of the flat core of their corresponding bis(β -diketonato)copper(II) complexes **3** and **4**. However, despite the columnar hexagonal arrangement observed in both compounds, complex **3**, having butoxyphenyl substituents, also exhibits layer-like characteristics not seen in **4**. Therefore, the phenoxyphenyl groups appear to be responsible for the absence of a layer-like structure as well as for the exhibited nonmesogenic behavior.

Experimental Part

General. All commercial reagents were used as supplied. The reaction solvents were degassed prior to use. FT-IR Spectra: Nicolet Magna-IR-550 spectrophotometer; KBr pellets; 4000–350 cm^{-1} region; in cm^{-1} . FAB-MS: VG-AutoSpec spectrometer; m/z (rel. %). ^1H - and $^{13}\text{C}\{^1\text{H}\}$ -NMR Spectra: Varian VXR-300 or Bruker AM-300 spectrophotometers of the NMR Service of the Complutense University; CDCl_3 solns.; chemical shifts δ in ppm rel. to SiMe_4 , with the signal of the deuterated solvent as reference, J in Hz. Elemental analyses (C, H, N) were carried out by the Microanalytical Service of the Complutense University.

Magnetic susceptibilities: SQUID magnetometer MPMS XL-5 manufactured by Quantum Design; at constant magnetic field of 1 T; 2–300 K temperature range. Phase studies: by optical microscopy with an Olympus BX50 microscope equipped with a Linkam THMS-600 heating stage; temp. assignment on the basis of optical observations with polarized light. Measurements of the transition temperatures: Perkin-Elmer Pyris-1 differential scanning calorimeter; samples (2–6 mg) were hermetically sealed in aluminium pans; heating or cooling rate 0.5–10°/min.

Ethyl 4-Butoxybenzoate. A mixture of 1-iodobutane (18.4 g, 0.1 mol), ethyl 4-hydroxybenzoate (18.28 g, 0.11 mol), and K_2CO_3 (20.73 g, 0.15 mol) in acetone (150 ml) was refluxed under continuous stirring for 2 d. Then, the mixture was cooled at r.t. and filtered and the inorg. residue extracted with CH_2Cl_2 (5×150 ml). The combined org. soln. was evaporated and the pale yellow oil distilled *in vacuo* at 130–135°: transparent viscous liquid (55%). ^1H -NMR (CDCl_3): 7.98, 6.88 ($2d, J = 9, \text{C}_6\text{H}_4$); 3.99 (t), 1.77 (qt), 1.46 (st), 0.97 ($t, J = 7, \text{Bu}$); 4.32 (q), 1.37 ($t, J = 7, \text{Et}$).

Ethyl 4-Phenoxybenzoate. To a soln. of 4-phenoxybenzoic acid (15 g, 0.07 mol) in EtOH (150 ml) was added 4 ml of sulfuric acid (spec. grav. 1.84). The mixture was refluxed for 3 d with stirring, then allowed to cool to r.t., and evaporated. The transparent oil obtained was distilled *in vacuo* at 167–168°: transparent viscous liquid (50%). ^1H -NMR (CDCl_3): 8.01, 6.99 ($2d, J = 9, \text{C}_6\text{H}_4$); 7.39 (t), 7.19 (t), 7.06 ($d, J = 8, \text{C}_6\text{H}_5$); 4.36 (q), 1.39 ($t, J = 7, \text{Et}$).

1,3-Bis(4-phenoxyphenyl)propane-1,3-dione (2). To a mixture of ethyl 4-phenoxybenzoate (8.25 g, 0.044 mol) and 4-phenoxyacetophenone (13.17 g, 0.063 mol) in THF (300 ml), a dispersion of 60% NaH in mineral oil (3.25 g, 0.135 mol) was added in small portions. When the effervescence ceased, the mixture was refluxed for 3 h with vigorous stirring. The mixture was allowed to cool to r.t. and then poured into H_2O (500 ml). Hydrochloric acid (spec. grav. 1.18) was added, giving rise to an orange oil that was extracted with Et_2O (5×150 ml). The combined extracts were evaporated and the resulting yellow solid recrystallized from CHCl_3 /hexane when the soln. was kept at 0° for several days: yellow needle-like crystals (53%). Anal. calc. for $\text{C}_{27}\text{H}_{20}\text{O}_4$: C 79.40, H 4.90; found: C 79.35, H 4.97.

1,3-Bis(4-butoxyphenyl)propane-1,3-dione (1). As described for **2**, but with dimethoxyethane as solvent (45 ml), ethyl 4-butoxybenzoate (5.53 g, 0.025 mol), 4-butoxyacetophenone (4.80 g, 0.025 mol), and 60% NaH dispersion (2.0 g, 0.083 mol): **1** as yellow prismatic-like crystals after recrystallization from MeCN (60%). Anal. calc. for $\text{C}_{23}\text{H}_{26}\text{O}_4$: C 74.97, H 7.39; found: C 74.85, H 7.59.

Bis[1,3-bis(4-phenoxyphenyl)propane-1,3-dionato- $\kappa\text{O},\kappa\text{O}'$]copper(II) (4). A soln. of copper(II) acetate monohydrate (63 mg, 0.31 mmol) in the minimum volume of 96% EtOH was added dropwise to a soln. of **2** (204 mg, 0.5 mmol) in abs. EtOH (5 ml). A solid immediately formed. The resulting light-green mixture was stirred at r.t. for 1 h. The precipitate was filtered, washed with H_2O and recrystallized from CH_2Cl_2 /hexane: **4** as a green needle-like solid (86%). IR (KBr): 1586 (br., CO, CC). Anal. calc. for $\text{C}_{54}\text{H}_{38}\text{CuO}_8$: C 73.83, H 4.32; found: C 73.35, H 4.25.

Bis[1,3-bis(4-butoxyphenyl)propane-1,3-dionato- $\kappa\text{O},\kappa\text{O}'$]copper(II) (3). As described for **4**, with copper(II) acetate monohydrate (63 mg, 0.31 mmol) and **1** (184 mg, 0.5 mmol): **3** as a deep-green needle-like solid

(72%). IR (KBr): 1603 (CO), 1586 (CC). FAB-MS: 798 (M^+). Anal. calc. for $C_{46}H_{46}CuO_8$: C 69.19, H 6.82; found: C 69.38, H 6.89.

X-Ray Diffraction Studies. Prismatic single crystals of **1**, **3**, and **4** were grown by layering CH_2Cl_2 with Et_2O . The crystal data are given in Table 4. The data were collected on a *Bruker Smart-CCD* diffractometer with graphite monochromated $MoK\alpha$ radiation (λ 0.71073 Å) operating at 50 kV and 20 mA. Data were collected over a hemisphere of the reciprocal space by combination of three exposure sets. Each exposure of 20 s covered 0.3° in ω . The cell parameters were determined and refined by least-squares fit of all reflections collected. The first 50 frames were recollected at the end of the data collection to monitor crystal decay, and no appreciable decay was observed.

Table 4. *Crystal and Refinement Data for 1, 3, and 4*

	1	3	4
Formula	$C_{23}H_{28}O_4$	$C_{46}H_{54}CuO_8$	$C_{54}H_{38}CuO_8$
<i>M</i>	368.45	798.43	878.38
Crystal system	Orthorhombic	Triclinic	Monoclinic
Space group	<i>Pccn</i>	$P\bar{1}$	$P2_1/n$
<i>a</i> /Å	36.574(3)	11.4653(1)	6.1533(1)
<i>b</i> /Å	9.6196(8)	17.2709(2)	12.0610(2)
<i>c</i> /Å	11.4699(9)	17.3234(2)	28.1931(1)
$\alpha/^\circ$		106.393(1)	
$\beta/^\circ$		91.666(1)	96.026(1)
$\gamma/^\circ$		100.714(1)	
<i>V</i> /Å ³	4035.4(6)	3221.37(6)	2080.79(5)
<i>Z</i>	8	3	2
<i>F</i> (000)	1584	1269	910
<i>D</i> /g cm ⁻³	1.21	1.24	1.40
Temp./K	296	296	296
μ (MoK α)/mm ⁻¹	0.082	0.559	0.585
Crystal size/mm	0.11 × 0.11 × 0.08	0.45 × 0.30 × 0.25	0.40 × 0.25 × 0.10
Scan technique	ω - ϕ	ω - ϕ	ω - ϕ
Data collected	(-28, -11, -13) to (43, 11, 13)	(-13, -20, -15) to (13, 20, 20)	(-7, -7, -37) to (8, 16, 37)
$\theta/^\circ$	2.19–25.00	1.23–25.00	1.45–28.29
Refls. collected	16152	17450	13483
Unique refls.	3511	11098	5115
	(R_{int} = 0.070)	(R_{int} = 0.0246)	(R_{int} = 0.0433)
Data, restraints, parameters	3511, 0, 249	11098, 138, 745	5115, 0, 286
G.o.f. (F^2)	0.847	1.04	0.79
<i>R</i> ($I \geq 2\sigma(I)$) ^a	0.045 (1529 refls.)	0.065 (7484 refls.)	0.049 (3494 refls.)
<i>Rw</i> _F ^b	0.10	0.22	0.16

^a) $\Sigma[|F_o| - |F_c|]/\Sigma|F_o|$. ^b) $(\Sigma[w(F_o^2 - F_c^2)^2]/\Sigma[w(F_o^2)^2])^{1/2}$.

The structures of **1** and **4** were solved by direct and *Fourier* methods, and **3** by *Patterson* and *Fourier* techniques.

The refinement for the three structures was made by full-matrix least-squares on F^2 [34]. All non-H-atoms were refined anisotropically. The H-atoms were calculated and refined as riding on the C-bonded atom with a common anisotropic displacement, except the H-atom bonded to O(2) in **1**, which was located in a difference *Fourier* synthesis, included, and refined its coordinates. For **3**, all C-atoms in the chains were refined with restraints for anisotropic thermal parameters because a nonresolvable positional disorder was found for these chains.

The largest residual peaks in the final difference map were 0.12, 1.62, and 0.50 for **1**, **3**, and **4**, resp., close to the C-atoms of the chains. The refinement converged to *R* values of 0.045 (1529 observed reflections), 0.065

(7484 observed reflections), and 0.049 (3494 observed reflections) for **1**, **3**, and **4** resp. The supplementary crystallographic data have been deposited at the *Cambridge Crystallographic Data Centre* (CCDC deposition numbers 152856–152858).

We thank the *DGES* of Spain for financial support (Projects No. PB95-0370 and PB98-0766).

REFERENCES

- [1] S. A. Hudson, P. M. Maitlis, *Chem. Rev.* **1993**, *93*, 861.
- [2] P. Espinet, M. A. Esteruelas, L. A. Oro, J. L. Serrano, E. Sola, *Coord. Chem. Rev.* **1992**, *117*, 215.
- [3] A. M. Giroud-Godquin, P. M. Maitlis, *Angew. Chem., Int. Ed.* **1991**, *30*, 375.
- [4] 'Metallomesogens, Synthesis, Properties, and Applications', Ed. J. L. Serrano, VCH Publishers, New York, 1996.
- [5] V. Bezborodov, R. Dabrowski, *Mol. Cryst. Liq. Cryst.* **1997**, *299*, 1.
- [6] K. Ohta, Y. Inagaki-Oka, H. Hasebe, I. Yamamoto, *Polyhedron* **2000**, *19*, 267, and ref. cit. therein.
- [7] X. Yang, Q. Lu, S. Dong, D. Liu, S. Zhu, F. Wu, R. Zhang, *J. Phys. Chem.* **1993**, *97*, 6726.
- [8] H. Sakashita, A. Nishitani, Y. Sumiya, H. Terauchi, K. Ohta, I. Yamamoto, *Mol. Cryst. Liq. Cryst.* **1988**, *163*, 211.
- [9] A. M. Giroud-Godquin, M. M. Gauthier, G. Sigaud, F. Hardouin, M. F. Achard, *Mol. Cryst. Liq. Cryst.* **1986**, *132*, 35.
- [10] A. M. Godquin-Giraud, G. Sigaud, M. F. Achard, F. Hardouin, *J. Phys. Lett.* **1984**, *45*, L387.
- [11] W. Haase, M. A. Athanassopoulou, *Struct. Bond.* **1999**, *94*, 139.
- [12] S. Tantrawong, P. Styring, *Mol. Cryst. Liq. Cryst.* **1997**, *302*, 309.
- [13] C. Cativiela, J. L. Serrano, M. M. Zurbano, *J. Org. Chem.* **1995**, *60*, 3074.
- [14] S. C. Trzaska, T. M. Swager, *Chem. Mater.* **1998**, *10*, 438.
- [15] J. Barberá, C. Cativiela, J. L. Serrano, M. M. Zurbano, *Adv. Mat.* **1991**, *3*, 602.
- [16] K. Ohta, A. Ishii, I. Yamamoto, K. Matsuzaki, *J. Chem. Soc., Chem. Commun.* **1984**, 1099.
- [17] K. Ohta, H. Muroki, K. I. Hatada, I. Yamamoto, K. Matsuzaki, *Mol. Cryst. Liq. Cryst.* **1985**, *130*, 249.
- [18] K. Ohta, A. Ishii, A. Muroki, I. Yamamoto, K. Matsuzaki, *Mol. Cryst. Liq. Cryst.* **1985**, *116*, 299.
- [19] K. Ohta, H. Muroki, A. Takagi, K. Hatada, H. Ema, I. Yamamoto, K. Matsuzaki, *Mol. Cryst. Liq. Cryst.* **1986**, *140*, 131.
- [20] H. Sakashita, A. Nishitani, Y. Sumiya, H. Terauchi, K. Ohta, I. Yamamoto, *Mol. Cryst. Liq. Cryst.* **1988**, *163*, 211.
- [21] A. B. Blake, J. R. Chipperfield, S. Clark, P. G. Nelson, *J. Chem. Soc., Dalton Trans.* **1991**, 1159.
- [22] H. Zheng, C. K. Lai, T. M. Swager, *Chem. Mater.* **1995**, *7*, 2067.
- [23] H. Zheng, B. Xu, T. M. Swager, *Chem. Mater.* **1996**, *8*, 907.
- [24] K. Usha, K. Vijayan, B. K. Sadashiva, *Mol. Cryst. Liq. Cryst. Lett.* **1987**, *5*, 67.
- [25] K. Usha, K. Vijayan, *Mol. Cryst. Liq. Cryst.* **1989**, *174*, 39.
- [26] K. Usha, K. Vijayan, B. K. Sadashiva, *Mol. Cryst. Liq. Cryst.* **1991**, *201*, 13.
- [27] K. Usha, K. Vijayan, *Mol. Cryst. Liq. Cryst.* **1992**, *220*, 77.
- [28] K. Usha, K. Vijayan, *Liq. Cryst.* **1992**, *12*, 137.
- [29] B. Mühlberger, W. Haase, *Liq. Cryst.* **1989**, *5*, 251.
- [30] K. Ohta, H. Muroki, K. I. Hatada, A. Takagi, H. Ema, I. Yamamoto, K. Matsuzaki, *Mol. Cryst. Liq. Cryst.* **1986**, *140*, 163.
- [31] J. Barberá, C. Cativiela, J. L. Serrano, M. M. Zurbano, *Liq. Cryst.* **1992**, *11*, 887.
- [32] J. Barberá, R. Giménez, J. L. Serrano, R. Alcalá, B. Villacampa, J. Villalba, I. Ledoux, J. Zyss, *Liq. Cryst.* **1997**, *22*, 265.
- [33] M. C. Etter, D. A. Jahn, Z. Urbanczyk-Lipkowska, *Acta Crystallogr., Sect. C* **1987**, *43*, 260.
- [34] SHELXTL, Version 5.10, Bruker Analytical X-Ray Systems, 1997.

Received March 26, 2001